

Oversampled Low Ambiguity Zone Sequences for Channel Estimation over Doubly Selective Channels

Zhi Gu, Zhengchun Zhou, Pingzhi Fan, Avik Ranjan Adhikary, and Zilong Liu

Abstract—Pilot sequence design over doubly selective channels (DSC) is challenging due to the variations in both the time- and frequency-domains. Against this background, the contribution of this paper is twofold: Firstly, we investigate the optimal sequence design criteria for efficient channel estimation in orthogonal frequency division multiplexing systems under DSC. Secondly, to design pilot sequences that can satisfy the derived criteria, we propose a new metric called oversampled ambiguity function (O-AF), which considers both fractional and integer Doppler frequency shifts. Optimizing the sidelobes of O-AF through a modified iterative twisted approximation (ITROX) algorithm, we develop a new class of pilot sequences called “oversampled low ambiguity zone (O-LAZ) sequences”. Through numerical experiments, we evaluate the efficiency of the proposed O-LAZ sequences over the traditional low ambiguity zone (LAZ) sequences, Zadoff-Chu (ZC) sequences and m-sequences, by comparing their channel estimation performances over DSC.

Index Terms—Ambiguity function, channel estimation, doubly selective channel, ITROX algorithm, orthogonal frequency division multiplexing (OFDM), oversampled ambiguity zone (O-AZ) sequences.

I. INTRODUCTION

There is a growing research interest in high-mobility and high-rate wireless communications, such as those utilized in high-speed train and Vehicle-to-Everything (V2X) communications, as well as low-earth-orbit satellite networks [1]–[5]. These communications typically occur over doubly selective channels (DSC), which are challenging due to the time and frequency selectivity caused by multipath propagation and Doppler shifts/spread. Interference suppression in DSC is one of the main challenges faced by modern communication systems.

Orthogonal Frequency-Division Multiplexing (OFDM) systems have been successfully incorporated into important standards like the 3rd Generation Partnership Project (3GPP) Long Term Evolution (LTE), New Radio (NR), and IEEE 802.11a/g/n/ac/ax due to their excellent spectral efficiency, robustness to multipath fading, and low implementation complexity [6], [7]. However, in DSC, OFDM systems suffer from severe inter-carrier interference (ICI), which becomes more severe with increasing speed and carrier frequency. This interference negatively impacts the accuracy of channel estimation and the correctness of data demodulation. Extensive research has been conducted on channel estimation in DSC for OFDM systems. For example, researchers have proposed conditions for the orthogonality between pilot and data symbols at the channel output [8]. Based on this orthogonality condition, frequency-domain Kronecker delta (FDKD) pilots have been considered for frequency-domain pilot designs [9]–

[11]. However, these schemes often require specific modifications to the OFDM frame structure, limiting their practical application. Although recursive channel estimation algorithms offer good ICI mitigation capabilities, they typically come with drawbacks such as high computational complexity and the need for detailed channel statistical information [12]–[15]. These challenges make it difficult to apply these methods within LTE/NR standards.

In light of these challenges, achieving ICI suppression and accurate channel estimation with low complexity, without altering the existing LTE/NR frame structure, remains a hot research topic in the industry. This paper focuses on designing pilot sequences for channel estimation in DSCs to mitigate ICI, without requiring changes to the frame structure or channel estimation algorithms in LTE/NR. This approach enhances the robustness of the proposed sequences for practical engineering applications.

Zero/Low Correlation Zone (ZCZ/LCZ) sequences and Zero/Low Ambiguity Zone (ZAZ/LAZ) sequences are among the traditional sequences in sequence design. Sequences with good correlation properties have found many applications in modern communication systems [16]–[18]. In practice, sequences with zero correlation sidelobes in all delays are preferred, but achieving this is generally difficult. Given the quasi-synchronous nature of communication systems, the concept of ZCZ sequences was first introduced in 1999 [19], followed by LCZ sequences, where sidelobes within the LCZ region are bounded by a small positive value. Theoretical bounds for ZCZ and LCZ sequences under periodic correlation are derived in [20].

The relative movement between the transmitter and receiver causes signal distortion, known as the Doppler effect. The ambiguity function (AF) is used to measure Doppler frequency shifts and helps determine relative velocity in radar systems. An AF of a sequence \mathbf{a} , denoted by $AF_{\mathbf{a}}(\tau, f)$, is a two-dimensional function of the propagation delay (τ) and the Doppler shift (f) [21]. The correlation of a sequence gives the AF of the sequence along the zero-Doppler axis. However, similar to the correlation function, it is impossible to maintain zero AF sidelobes for all non-zero Doppler shifts. Therefore, the concepts of ZAZ and LAZ sequences were introduced [22], with theoretical bounds derived for these sequences under periodic correlation [23].

Systematic constructions of sequences with various correlation properties are typically based on algebraic tools [19], [23]–[31] or optimization algorithms. Algebraic constructions are straightforward to implement but often result in sequences with limited parameters. In contrast, optimization-based meth-

ods offer more flexibility [22], [32], though they generally come with higher complexity. Notably, in 2004, Deng [33] proposed an algorithm that combined simulated annealing with heuristic search to suppress sidelobes of global aperiodic correlation, marking the start of sequence design based on algorithmic methods.

Due to the high complexity of heuristic search algorithms, researchers have developed new sequence generation algorithms based on optimization theory. Examples include the Cyclic-Algorithm-Original (CAO), proposed in 2008, aiming to reduce periodic/aperiodic correlation sidelobes through SVD decomposition of the correlation matrix [34]. Subsequently Cyclic-algorithm-new (CAN) algorithm [35], [36], based on alternating minimization techniques, was designed to synthesize unimodular aperiodic sequences of large length. However, its drawback is that the solution of the approximate problem does not always converge to the minimum of the original problem. The Monotonic minimizer for integrated sidelobe level (MISL) [37] algorithm utilizes the majorization-minimization (MM) method to minimize a surrogate function of the original integrated sidelobe level (ISL) minimization problem, ensuring convergence to the global minima of the original problem. Nevertheless, its convergence is slow due to the double majorization of the original cost function. In recent years, efficient algorithms for generating unimodular sequences have emerged, such as Limited-Memory BFGS (LBFGS) [38], [39], Iterative Twisted Approximation (ITROX) computational framework [40]–[42], Power Spectral Density Fitting-based Iterative Approach (PIA) [43], Efficient Gradient Descent (EGD) [44], Coordinate Descent (CD) [45], Alternating Direction Method of Multipliers (ADMM), Parallel Direction Method of Multipliers (PDMM) [46], algorithm based on neural networks [47]. Most of the algorithms mentioned above focus on achieving better suppression levels for correlation sidelobes than the earlier methods could achieve [48]–[52]. Due to space limitation, these methods are not discussed in details here. In Table I, we give an overview of relevant sequence design algorithms that can design sequences with low correlations, for comparison. Here, we only present the complexity of the correlation optimization problem for a single sequence of length N and LCZ width Z .

TABLE I
COMPARISON OF LCZ SEQUENCE DESIGN ALGORITHMS

Algorithms	Computational Complexity	Aperiodic Correlation	Periodic Correlation
CAO [34]	$\mathcal{O}(NZ^2 + Z^3)$	✓	✓
CAN [35]	$\mathcal{O}(N^2)$	✓	×
PeCAN [36]	$\mathcal{O}(N^2)$	×	✓
LBFGS [39]	$\mathcal{O}(NZ + N \log_2 N)$	✓	×
ITROX [40]	$\mathcal{O}(N^3)$	✓	✓
PIA [43]	$\mathcal{O}(N^2)$	✓	×
MISL [37]	$\mathcal{O}(N^2)$	✓	✓
EGD [44]	$\mathcal{O}(N^2)$	✓	×

Similar to the generation of ZCZ/LCZ sequences, optimization-based algorithms are the primary methods for generating ZAZ/LAZ sequences. Additionally, some ZCZ/LCZ sequence generation methods can be adapted to improve ZAZ/LAZ sequence generation algorithms, such as

the AF-CAO [34]. Besides, there are many other optimization methods such as Maximum Block Improvement (MBI) method [53], gradient descent (GD) [54], coordinate iteration for ambiguity function iterative shaping (CIAFIS) [55], accelerated iterative sequential optimization (AISO) algorithm [56], [57], Lagrange programming neural network-alternating direction method of multipliers (LPNN-ADMM) [58], quartic GD [59], projected GD, manifold optimization embedding with momentum (MOEM), LBFGS, etc [60]–[62]. Although GD-based algorithms are generally effective, they tend to be slow due to the need to calculate gradients at every step. In Table II, we give an overview of relevant sequence design algorithms that can design sequences with low ambiguity, for comparison. Again, we only present the complexity of the ambiguity optimization problem for a single sequence of length N and LAZ size $Z \times F$.

TABLE II
COMPARISON OF LAZ SEQUENCE DESIGN ALGORITHMS

Algorithms	Computational Complexity	Aperiodic AF	Periodic AF
AF-CAO [34]	$\mathcal{O}((N + Z)Z^2F^2)$	✓	✓
MBIL [53]	$\mathcal{O}(N)$	✓	×
MBIQ [53]	$\mathcal{O}(N^{3.5})$	✓	×
GD [54]	$\mathcal{O}(N^2F)$	✓	✓
CIAFIS [55]	$\mathcal{O}(N^2)$	✓	×
AISO [56], [57]	Not report	✓	×
LPNN-ADMM [58]	$\mathcal{O}(N^2ZF)$	✓	×

These ZCZ/LCZ/ZAZ/LAZ sequences offer the advantages of flexible length and adaptable ZCZ and ZAZ sizes, making them suitable for various applications, including radar waveform design [34], [63]. Channel estimation, which involves separating time delay and Doppler shift, is conceptually similar to radar’s velocity and range measurement. Motivated by this similarity, this paper explores the use of ZAZ/LAZ sequences as pilot sequences for channel estimation in DSC.

Contributions: To develop efficient preamble sequences in OFDM, we first analyze the requirements for pilot sequences in DSC channel estimation. Based on the Jakes’ model of the Rayleigh fading channel (to be detailed in Section III), we observe that Doppler shifts in DSC can be non-integer, which limits the effectiveness of conventional ZAZ and LAZ sequences. To address this issue, we introduce the concept of oversampled ambiguity functions (O-AF) for more accurate estimation of channel responses at both integer and fractional Doppler shifts. This concept leads to the development of oversampled zero/low ambiguity zone (O-ZAZ/O-LAZ) sequences.

Similar to traditional ZAZ/LAZ, we coin the concept of oversampled zero/low ambiguity zone (O-ZAZ/O-LAZ) if there is a region in the ambiguity plot with zero/low sidelobes. Through a series of trial and error (as detailed in Remark 6), we chose the traditional ITROX algorithm and modify it to design O-LAZ sequences. We named the modified ITROX algorithm as oversampled ambiguity ITROX (OA-ITROX) algorithm. The major difference between OA-ITROX with the traditional ITROX is that, here we incorporate submatrices with frequency offsets and have replaced eigenvalue decomposition (EVD) with SVD. The proposed OA-ITROX

algorithm is capable of designing both traditional LAZ as well as O-LAZ sequences. It is shown that the complexity of OA-ITROX highly depends on SVD. We further address the complexity of OA-ITROX by employing the power method for rank-1 approximation instead of SVD (as shown in *Remark 5*). Finally, numerical experiments demonstrate that sequences with low O-AF properties can be effectively used as pilot sequences for channel estimation in DSC.

Organization: The rest of the paper is organized as follows. Section II introduces the notations and discusses ZCZ/LCZ and ZAZ/LAZ sequences, followed by an overview of OFDM system principles and channel estimation. In Section III, we revisit the Jakes' model and analyze its impact on signals, leading to the derivation of design criteria for pilot sequences in DSC. Section IV presents the OA-ITROX algorithm and the designed O-LAZ sequences. Section V evaluates the proposed training scheme through simulations. Finally, Section VI concludes the paper.

II. PRELIMINARIES

The following notations will be used throughout this paper.

- \mathbf{X}^* , \mathbf{X}^T and \mathbf{X}^H denote the complex conjugate, the transpose and the conjugate transpose of matrix \mathbf{X} , respectively;
- $\langle \mathbf{a}, \mathbf{b} \rangle$ denotes the inner-product between two complex valued sequences $\mathbf{a} = [a[0], a[1], \dots, a[N-1]]^T$, $\mathbf{b} = [b[0], b[1], \dots, b[N-1]]^T$, i.e., $\langle \mathbf{a}, \mathbf{b} \rangle = \sum_{k=0}^{N-1} a[k]b^*[k]$, where N is the sequence length of \mathbf{a} (and \mathbf{b});
- $[\mathbf{a}]_k$ denotes the k -th element of sequence \mathbf{a} ;
- $[\mathbf{X}]_{i,j}$ denotes the i -th row j -th column element of matrix \mathbf{X} ;
- $S^\tau(\mathbf{a})$ denotes the right-cyclic-shift of $\mathbf{a} = [a[0], a[1], \dots, a[N-1]]^T$ for τ (nonnegative integer) positions, i.e.,

$$S^\tau(\mathbf{a}) = \underbrace{[a[N-\tau], \dots, a[N-1], a[0], a[1], \dots, a[N-\tau-1]]^T}_{\text{the last } \tau \text{ elements of } \mathbf{a}}$$

Similarly,

$$S^{-\tau}(\mathbf{a}) = [a[\tau], a[\tau+1], \dots, a[N-1], \underbrace{a[0], a[1], \dots, a[\tau-1]}_{\text{the first } \tau \text{ elements of } \mathbf{a}}]^T;$$

- $[n]_N$ denotes $n \pmod{N}$;
- ζ_N denotes the N -th complex roots of unity, i.e., $\zeta_N = e^{2\pi i/N}$;
- \mathbf{F}_N denotes the Fourier matrix of size N , i.e., $[\mathbf{F}_N]_{i,j} = \frac{1}{\sqrt{N}} \zeta_N^{-(i-1)(j-1)}$;
- $\mathbf{a} \odot \mathbf{b}$ denotes elementwise multiplication, i.e., $[\mathbf{a} \odot \mathbf{b}]_k = a[k]b[k]$;
- $\mathbf{a} \oslash \mathbf{b}$ denotes elementwise division, i.e., $[\mathbf{a} \oslash \mathbf{b}]_k = a[k]/b[k]$;
- $\text{mean}(\mathbf{a})$ denotes the mean of \mathbf{a} , i.e., $\text{mean}(\mathbf{a}) = (\sum_{k=0}^{N-1} a[k])/N$;
- $\varphi(\mathbf{a})$ denotes the phase of each of the elements of \mathbf{a} ;
- $E(\cdot)$ denotes the expected value of a random variable.

For two length- N complex-valued sequences $\mathbf{a} = [a[0], a[1], \dots, a[N-1]]^T$, $\mathbf{b} = [b[0], b[1], \dots, b[N-1]]^T$, $\phi_{\mathbf{a},\mathbf{b}}(\tau)$ denotes the periodic cross-correlation function (PCCF) between \mathbf{a} and \mathbf{b} , i.e.,

$$\phi_{\mathbf{a},\mathbf{b}}(\tau) = \sum_{k=0}^{N-1} a[k]b^*[[k+\tau]_N] = \langle \mathbf{a}, S^{-\tau}(\mathbf{b}) \rangle. \quad (1)$$

In particular, when $\mathbf{a} = \mathbf{b}$, $\phi_{\mathbf{a},\mathbf{b}}(\tau)$ is written as $\phi_{\mathbf{a}}(\tau)$ and called the periodic auto-correlation function (PACF) of \mathbf{a} at time-shift τ .

For two length N complex-valued sequences $\mathbf{a} = [a[0], a[1], \dots, a[N-1]]^T$, $\mathbf{b} = [b[0], b[1], \dots, b[N-1]]^T$, $AF_{\mathbf{a},\mathbf{b}}(\tau, f)$ denotes the periodic cross-ambiguity function (PCAF) between \mathbf{a} and \mathbf{b} at time-shift τ and frequency-shift f , i.e.,

$$AF_{\mathbf{a},\mathbf{b}}(\tau, f) = \sum_{k=0}^{N-1} a[k]b^*[[k+\tau]_N] \zeta_N^{fk} = \langle \mathbf{a} \odot \mathbf{f}, S^{-\tau}(\mathbf{b}) \rangle, \quad (2)$$

where $\mathbf{f} = [1, \zeta_N^f, \dots, \zeta_N^{f(N-1)}]^T$. In particular, when $\mathbf{a} = \mathbf{b}$, $AF_{\mathbf{a},\mathbf{b}}(\tau, f)$ is written as $AF_{\mathbf{a}}(\tau, f)$ and called the periodic auto-ambiguity function (PAAF) of \mathbf{a} at time-shift τ and frequency-shift f .

Remark 1: Note that in (1) and (2), the values of τ and f are integers, i.e., $\tau, f = 0, 1, \dots, N-1$.

A. Zero/Low Correlation/Ambiguity Zone Sequence

Next, we give a brief introduction to zero/low correlation/ambiguity zone sequence. Integrated sidelobe level (ISL) is an important metric, which is used to characterize the correlation and AF of sequences.

Definition 1: Let $\mathbf{a} = [a[0], a[1], \dots, a[N-1]]^T$ be a sequence of length N , the ISL of correlation is define by

$$\text{ISL}_\phi(\mathbf{a}; Z) = 2 \sum_{\tau=1}^Z |\phi_{\mathbf{a}}(\tau)|^2, \quad (3)$$

where Z is the size of concerned correlation zone. Similarly, the ISL of AF is define by

$$\text{ISL}_{AF}(\mathbf{a}; Z \times F_r) = 2 \sum_{\tau=1}^Z \sum_{f=-F_r}^{F_r} |AF_{\mathbf{a}}(\tau, f)|^2, \quad (4)$$

where $Z \times F_r$ is the size of concerned ambiguity zone.

By the above definition of ISL, we can give the definitions of zero correlation/ambiguity zone sequence.

Definition 2: A sequence \mathbf{a} of length N is called a zero correlation zone (ZCZ) sequence with ZCZ width Z , if

$$\text{ISL}_\phi(\mathbf{a}; Z) = 0. \quad (5)$$

Similarly, \mathbf{a} is called a zero ambiguity zone (ZAZ) sequence with ZAZ size $Z \times F_r$, if

$$\text{ISL}_{AF}(\mathbf{a}; Z \times F_r) = 0. \quad (6)$$

Designing sequences which satisfy conditions (5) and (6) are very challenging. Low correlation/ambiguity zone is generalized version of ZCZ/ZAZ. Normally, it is required that ISL should be as low as possible.

Definition 3: A sequence \mathbf{a} of length N is called a low correlation zone (LCZ) sequence with LCZ width Z , if

$$\text{ISL}_\phi(\mathbf{a}; Z) < \varepsilon, \quad (7)$$

where ε is a very small value.

Similarly, \mathbf{a} is called a low ambiguity zone (LAZ) sequence with LAZ size $Z \times F_r$, if

$$\text{ISL}_{AF}(\mathbf{a}; Z \times F_r) < \varepsilon. \quad (8)$$

B. System Model of OFDM and Channel Estimation

In this paper, we consider an OFDM transmission system with N carriers. To simplify the system model, we assume that both the transmitter and receiver have a single antenna. Fig. 1 shows the transmission frame structure of the OFDM system. Within a frame, we assume a total of M_P pilot OFDM

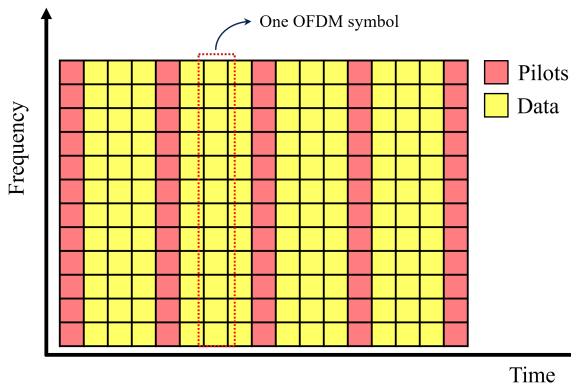


Fig. 1. The transmission frame structure.

symbols, with each pair of pilot OFDM symbols containing M_D data OFDM symbols. Consequently, an OFDM frame comprises a total of $M = M_P + M_D(M_P - 1)$ OFDM symbols.

For the m -th OFDM symbol, the time-domain received signal after removing the cyclic prefix can be represented as $\mathbf{y}_m = [y_m[0], y_m[1], \dots, y_m[N-1]]^T$, $m = 0, 1, \dots, M-1$, and it can be expressed as:

$$y_m[n] = \sum_{l=0}^{L-1} h_m[l, n] x_m[[n-l]_N] + w_m[n],$$

where $\mathbf{x}_m = [x_m[0], x_m[1], \dots, x_m[N-1]]^T$ represents the m -th OFDM symbol in the time-domain. $h_m[l, n]$ is the channel response matrix of m -th OFDM symbol in the time-domain. Channel estimation is first performed over pilot OFDM symbols and then discrete prolate spheroidal sequences (DPSS) interpolation is used to achieve channel estimation over the data symbols [64].

Without loss of generality, we consider the channel estimation model for a single pilot OFDM symbol by least square (LS) method. Let $\mathbf{x} = \mathbf{a}$ be the time-domain sequence transmitted as the pilot OFDM symbols, then the LS estimation is given by

$$\hat{\mathbf{h}} = (\mathbf{A}_T^H \mathbf{A}_T)^{-1} \mathbf{A}_T^H \mathbf{y}, \quad (9)$$

where \mathbf{y} is the time-domain sequence received after removing the cyclic prefix, \mathbf{A}_T is the cyclic matrix of size $N \times L$ (L

is the maximum multipath delay) generated by \mathbf{a} , and it is defined as follows

$$\mathbf{A}_T = \begin{bmatrix} a[0] & a[N-1] & \cdots & a[N-L+1] \\ a[1] & a[0] & \cdots & a[N-L+2] \\ \vdots & \vdots & & \vdots \\ a[N-1] & a[N-2] & \cdots & a[N-L] \end{bmatrix}. \quad (10)$$

From (9), it can be observed that the channel estimation obtained by the LS method is a vector, representing an estimate of the true channel response at a certain instant. Mostofi *et al.* [65] proved that the channel estimated by the LS method corresponds to the estimate of the midpoint instant of the true channel response in the sense of statistical averaging [65].

Lemma 1 ([65]): Let $h[l, n]$ be the true channel response at the n -th instant and the l -th path corresponding to an OFDM symbol, and \mathbf{h}_n contains the channel response of all the L multipaths at n -th instant, i.e., $\mathbf{h}_n = [h[0, n], h[1, n], \dots, h[L-1, n]]^T$. The average channel response over the OFDM time duration of $n = [0, 1, \dots, N-1]$ is closest to the midpoint instant $\mathbf{h}_{\text{mid}} = \mathbf{h}_{\frac{N-1}{2}}$. This can be mathematically described as follows

$$E(\|\mathbf{h}_{\text{avg}} - \mathbf{h}_n\|^2) \text{ is minimized for } n = \frac{N-1}{2},$$

where $\mathbf{h}_{\text{avg}} = 1/N \sum_{n=0}^{N-1} \mathbf{h}_n$. Furthermore, the channel estimation values $\hat{\mathbf{h}}$ obtained by the LS method are estimated of the average channel response, i.e., $\hat{\mathbf{h}} = \hat{\mathbf{h}}_{\text{avg}}$. And it is also close to the midpoint instant of actual channel response,

$$E(\|\hat{\mathbf{h}} - \mathbf{h}_n\|^2) \text{ is minimized for } n = \frac{N-1}{2}.$$

III. OPTIMAL PILOT DESIGN CRITERION FOR DSC

Jakes model has become a well-established benchmark in the research community due to its realistic Doppler spectrum representation, which accurately models the frequency variations caused by the relative motion between the transmitter and receiver [66]. In this section, we first revisit the Jakes' channel model for DSC. Then we derive the optimal pilot design criterion for the channel model.

Jakes' Model for DSC: Here we consider the case of a single OFDM symbol with N subcarriers. The time-domain received sequence after removing the cyclic prefix can be represented as $\mathbf{y} = [y[0], y[1], \dots, y[N-1]]^T$ which can be expressed as follows:

$$y[n] = \sum_{l=0}^{L-1} h[l, n] x[[n-l]_N] + w[n], \quad (11)$$

where L denotes the number of delay paths, $\mathbf{x} = [x[0], x[1], \dots, x[N-1]]^T$ represents the time-domain transmitted sequence, and $h[l, n]$ is an element of time-domain channel response matrix, which represents the channel at the n -th sampling time on the l -th multipath. The improved Jakes' simulator [66] by sum-of-sinusoids statistical simulation models is given by

$$h[l, t] = E_0 \sum_{q=0}^{Q-1} A_l C_q^{(l)} e^{i(2\pi f_a t \cos \alpha_q^{(l)} + \phi_q^{(l)})}, \quad (12)$$

where

$$\begin{aligned} C_q^{(l)} &= \frac{e^{i\psi_q^{(l)}}}{\sqrt{Q}}, q = 0, 1, \dots, Q-1, \\ \alpha_q^{(l)} &= \frac{2\pi q - \pi + \theta^{(l)}}{Q}, q = 0, 1, \dots, Q-1, \\ \phi_q^{(l)} &= \phi_{Q/2+q}^{(l)} = \tilde{\phi}_q^{(l)}, q = 0, 1, \dots, Q/2-1, \end{aligned}$$

Q denotes the number of Doppler paths of each delay path and it is assumed to be even, E_0 the scaling constant, f_d the maximum Doppler frequency, A_l denotes the power of the the l -th path and follows complex Gaussian distribution with a mean of zero and a variance of $\sqrt{P_l}$, and $\psi_q^{(l)}$, $\theta^{(l)}$ and $\tilde{\phi}_q^{(l)}$ being mutually independent random variables uniformly distributed over $[-\pi, \pi]$.

Note that in OFDM, the received signal is discretely sampled from the interval $[0, T_s]$, i.e., $t = nT_s/N$, $n = 0, 1, \dots, N-1$, where T_s denotes the OFDM symbol duration. Let F_r denote the normalized maximum Doppler frequency, i.e., $F_r = f_d/\Delta f = f_dT_s$, then (12) can be written as

$$\begin{aligned} h[l, n] &= E_0 \sum_{q=0}^{Q-1} A_l C_q^{(l)} e^{i(2\pi F_r n/N \cos \alpha_q^{(l)} + \phi_q^{(l)})} \\ &= E_0 \sum_{q=0}^{Q-1} A_l C_q^{(l)} e^{i\phi_q^{(l)}} e^{2\pi i/N (F_r n \cos \alpha_q^{(l)})} \\ &= E_0 \sum_{q=0}^{Q-1} A_l C_q^{(l)} e^{i\phi_q^{(l)}} \zeta_N^{F_r \cos \alpha_q^{(l)} n}. \end{aligned} \quad (13)$$

By aggregating the random variables and neglecting the impact of large-scale fading, (13) becomes

$$h[l, n] = \sum_{q=0}^{Q-1} g_q^{(l)} \zeta_N^{\omega_q^{(l)} n}, \quad (14)$$

where $g_q^{(l)} = A_l C_q^{(l)} e^{i\phi_q^{(l)}}$, and $\omega_q^{(l)} = F_r \cos \alpha_q^{(l)}$. Note that from (14), it can be observed that the range of $\omega_q^{(l)}$ is in $[-F_r, F_r]$, and they are independently and identically distributed.

A. Optimal Pilot Design Criterion

In this subsection, we derive the optimal pilot design criterion over DSC. Substituting (14) in (11), we obtain the transmission model for OFDM as follows

$$y[n] = \sum_{l=0}^{L-1} \sum_{q=0}^{Q-1} g_q^{(l)} \zeta_N^{\omega_q^{(l)} n} x[[n-l]_N] + w[n]. \quad (15)$$

Let $\mathbf{x} = \mathbf{a}$ be the pilot sequence. For the ease of analysis, (15) can be represented in matrix form as follows:

$$\mathbf{y} = \sum_{q=0}^{Q-1} (\mathbf{A}_T \odot \mathbf{\Omega}_q) \mathbf{g}_q + \mathbf{w}, \quad (16)$$

where $\mathbf{g}_q = [g_q^{(0)}, g_q^{(1)}, \dots, g_q^{(L-1)}]^T$, \mathbf{A}_T is the cyclic matrix of size $N \times L$ generated by \mathbf{a} , as given in (10) and $\mathbf{\Omega}_q$ is

the Vandermonde matrix of size $N \times L$ generated by $\omega_q^{(l)}$, as follows:

$$\mathbf{\Omega}_q = \begin{bmatrix} \zeta_N^{\omega_q^{(0)}0} & \zeta_N^{\omega_q^{(1)}0} & \dots & \zeta_N^{\omega_q^{(L-1)}0} \\ \zeta_N^{\omega_q^{(0)}1} & \zeta_N^{\omega_q^{(1)}1} & \dots & \zeta_N^{\omega_q^{(L-1)}1} \\ \vdots & \vdots & \ddots & \vdots \\ \zeta_N^{\omega_q^{(0)}(N-1)} & \zeta_N^{\omega_q^{(1)}(N-1)} & \dots & \zeta_N^{\omega_q^{(L-1)}(N-1)} \end{bmatrix}.$$

Then the LS estimation is given by

$$\begin{aligned} \hat{\mathbf{h}} &= (\mathbf{A}_T^H \mathbf{A}_T)^{-1} \mathbf{A}_T^H \mathbf{y} \\ &= (\mathbf{A}_T^H \mathbf{A}_T)^{-1} \mathbf{A}_T^H \left(\sum_{q=0}^{Q-1} (\mathbf{A}_T \odot \mathbf{\Omega}_q) \mathbf{g}_q + \mathbf{w} \right) \\ &= \sum_{q=0}^{Q-1} (\mathbf{A}_T^H \mathbf{A}_T)^{-1} \mathbf{A}_T^H (\mathbf{A}_T \odot \mathbf{\Omega}_q) \mathbf{g}_q + (\mathbf{A}_T^H \mathbf{A}_T)^{-1} \mathbf{A}_T^H \mathbf{w}. \end{aligned} \quad (17)$$

Using Lemma 1, $\hat{\mathbf{h}}$ is an estimate of \mathbf{h}_{avg} . The corresponding MSE is

$$\text{MSE}_{\text{avg}} = E(\|\hat{\mathbf{h}} - \mathbf{h}_{\text{avg}}\|^2). \quad (18)$$

By substituting (17) into (18), we can derive the intrinsic relationship between MSE and the pilot sequence, given in (19), where

$$\mathbf{\Gamma}_q = \begin{bmatrix} \frac{1}{N} \sum_{n=0}^{N-1} \zeta_N^{\omega_q^{(0)} n} \\ \frac{1}{N} \sum_{n=0}^{N-1} \zeta_N^{\omega_q^{(1)} n} \\ \vdots \\ \frac{1}{N} \sum_{n=0}^{N-1} \zeta_N^{\omega_q^{(L-1)} n} \end{bmatrix}. \quad (20)$$

From traditional channel estimation theory, we know that the matrix $\mathbf{A}_T^H \mathbf{A}_T$ is required to be an identity matrix of order N [67] for minimum MSE. Hence, we get the first criterion (CR₁) of pilot design over DSC as follows:

$$\arg \min_{\mathbf{a}} \|\mathbf{A}_T^H \mathbf{A}_T - N \mathbf{I}_L\|_F^2, \quad (21)$$

where \mathbf{I}_L is an identity matrix of size $L \times L$.

Furthermore, from (19), the LS estimator is unbiased if the pilot sequence satisfies

$$(\mathbf{A}_T^H \mathbf{A}_T)^{-1} \mathbf{A}_T^H (\mathbf{A}_T \odot \mathbf{\Omega}_q) - \text{diag}(\mathbf{\Gamma}_q) = \mathbf{0}_L,$$

for all $q = 0, 1, \dots, Q-1$.

Note that an efficient pilot sequence should work in a variety of channels. Hence, the second criterion (CR₂) of pilot design is as follows:

$$\arg \min_{\mathbf{a}} \left\| (\mathbf{A}_T^H \mathbf{A}_T)^{-1} \mathbf{A}_T^H (\mathbf{A}_T \odot \mathbf{\Omega}_q) - \text{diag}(\mathbf{\Gamma}_q) \right\|_F^2, \quad (22)$$

where $\mathbf{\Gamma}_q$ is given in (20) and $\omega_q^{(l)} \in [-F_r, F_r]$.

To simplify the optimization algorithm, we replace CR₁ and CR₂ comprehensively with ISL of O-AF as follows:

$$\arg \min_{\mathbf{a}} \sum_{\substack{\tau=-Z \\ \tau \neq 0}}^Z \int_{-F_r}^{F_r} |\widetilde{AF}_{\mathbf{a}}(\tau, f)|^2 df, \quad (23)$$

$$\begin{aligned}
 \text{MSE}_{\text{avg}} &= E \left(\left\| \sum_{q=0}^{Q-1} (\mathbf{A}_T^H \mathbf{A}_T)^{-1} \mathbf{A}_T^H (\mathbf{A}_T \odot \boldsymbol{\Omega}_q) \mathbf{g}_q + (\mathbf{A}_T^H \mathbf{A}_T)^{-1} \mathbf{A}_T^H \mathbf{w} - \mathbf{h}_{\text{avg}} \right\|^2 \right) \\
 &= E \left(\left\| \sum_{q=0}^{Q-1} [(\mathbf{A}_T^H \mathbf{A}_T)^{-1} \mathbf{A}_T^H (\mathbf{A}_T \odot \boldsymbol{\Omega}_q) - \text{diag}(\boldsymbol{\Gamma}_q)] \mathbf{g}_q + (\mathbf{A}_T^H \mathbf{A}_T)^{-1} \mathbf{A}_T^H \mathbf{w} \right\|^2 \right). \quad (19)
 \end{aligned}$$

Let us call this CR₃. A detail discussion about the relation between CR₁, CR₂, and CR₃ is given in Appendix I.

Thus a sequence needs to have a low ambiguity sidelobe within the region $[-Z, Z] \times [-F_r, F_r]$, where $f \in [-F_r, F_r]$ is a continuous variable and hence can take fractional values, to be used as a pilot sequence for optimal channel estimation in DSC. The sequences which satisfy this condition are termed as O-LAZ sequences in this paper. In the next section we will derive some properties of O-LAZ sequences and also propose a construction using a modified ITROX algorithm.

IV. O-LAZ SEQUENCE: PROPERTIES AND CONSTRUCTION

To design O-LAZ sequences, which are required for optimal channel estimation in DSC, we introduce a new metric called oversampled ambiguity function (O-AF), as traditional AF considers only integer Doppler shifts. Before proceeding further, we formally define O-AF as follows.

A. Oversampled Ambiguity Function (O-AF)

Definition 4: For two length N complex-valued sequences \mathbf{a} , \mathbf{b} , let $\widetilde{AF}_{\mathbf{a},\mathbf{b}}(\tau, f)$ denote the oversampled periodic cross-ambiguity function (O-PCAF) between \mathbf{a} and \mathbf{b} at time-shift τ and frequency-shift f . The $\widetilde{AF}_{\mathbf{a},\mathbf{b}}(\tau, f)$ is defined by

$$\widetilde{AF}_{\mathbf{a},\mathbf{b}}(\tau, f) = \sum_{k=0}^{N-1} a[k] b^*[[k + \tau]_N] \zeta_N^{fk} = \langle \mathbf{a} \odot \mathbf{f}, S^{-\tau}(\mathbf{b}) \rangle, \quad (24)$$

where $\mathbf{f} = [1, \zeta_N^f, \dots, \zeta_N^{f(N-1)}]^T$, $\tau \in \mathbb{Z}$, $f \in \mathbb{R}$. In particular, when $\mathbf{a} = \mathbf{b}$, $\widetilde{AF}_{\mathbf{a},\mathbf{b}}(\tau, f)$ is written as $\widetilde{AF}_{\mathbf{a}}(\tau, f)$ and called the oversampled periodic auto-ambiguity function (O-PAAF) of \mathbf{a} at time-shift τ and frequency-shift f .

Remark 2: Since the Doppler shift f is a continuous variable and delay shift τ is an integer in (23), we only considered oversampling the Doppler axis while defining O-AF. This helps us to accurately measure the channel estimation performance of the pilot sequence, under DSC.

Remark 3: As a generalization of AF, the O-AF has some special properties.

- When f in $\widetilde{AF}_{\mathbf{a}}(\tau, f)$ is taken as an integer, O-AF becomes traditional AF, i.e., $\widetilde{AF}_{\mathbf{a}}(\tau, f) = AF_{\mathbf{a}}(\tau, f)$ if $f \in \mathbb{Z}$.
- $\widetilde{AF}_{\mathbf{a}}(\tau, f)$ is a periodic function with respect to τ , i.e., $\widetilde{AF}_{\mathbf{a}}(\tau + kN, f) = \widetilde{AF}_{\mathbf{a}}(\tau, f)$ for any integer k .
- $AF_{\mathbf{a}}(\tau, f)$ and $\widetilde{AF}_{\mathbf{a}}(\tau, f)$ both have the constant volume property, i.e., $\sum_{\tau=0}^{N-1} \sum_{f=0}^{N-1} |AF_{\mathbf{a}}(\tau, f)|^2 = N^3$, $\sum_{\tau=0}^{N-1} \int_0^N |\widetilde{AF}_{\mathbf{a}}(\tau, f)|^2 df = N^3$.

- For any unimodular sequence \mathbf{a} , its O-AF can be determined on zero delay axis, i.e., $|\widetilde{AF}_{\mathbf{a}}(0, f)| = \frac{\sin(f\pi)}{\sin(f\pi/N)}$.

Sequences with zero/low oversampled ambiguity zone are very important for practical applications. In order to characterize the values of O-AF within the target zone, let us introduce the definition of the ISL of O-AF similar to (6).

Definition 5: Let $\mathbf{a} = [a[0], a[1], \dots, a[N-1]]^T$ be a sequence of length N , the ISL of O-AF is define by

$$\text{ISL}_{\widetilde{AF}}(\mathbf{a}; Z \times F_r) = \sum_{\substack{\tau=-Z \\ \tau \neq 0}}^Z \int_{f=-F_r}^{F_r} |\widetilde{AF}_{\mathbf{a}}(\tau, f)|^2 df, \quad (25)$$

where $Z \times F_r$ is the size of oversampled ambiguity zone.

Similarly, we can define oversampled zero/low ambiguity zone (O-ZAZ/O-LAZ) sequence.

Definition 6: A sequence \mathbf{a} of length N is called a oversampled zero ambiguity zone (O-ZAZ) sequence with O-ZAZ size $Z \times F_r$, if

$$\text{ISL}_{\widetilde{AF}}(\mathbf{a}; Z \times F_r) = 0. \quad (26)$$

Similarly, \mathbf{a} is called a oversampled low ambiguity zone (O-LAZ) sequence with low O-LAZ size $Z \times F_r$, if

$$\text{ISL}_{\widetilde{AF}}(\mathbf{a}; Z \times F_r) < \varepsilon, \quad (27)$$

where $\varepsilon > 0$ is a small constant.

In fast time-varying channel estimation, it is usually necessary to have Z greater than the maximum normalized multipath delay and F_r greater than the maximum normalized Doppler frequency shift (Detailed calculations are given in Section III). For example, let us consider the 5G scenario and the Extended Vehicular A Model (EVA) channel defined in 3GPP [68], assuming the number of subcarriers $N = 128$, the carrier frequency $f_c = 5.4\text{GHz}$, the interval of subcarriers $\Delta f = 15\text{KHz}$, maximum multipath delay $\tau_{\text{max}} = 2.5100\mu\text{s}$, maximum relative speed $v_{\text{max}} = 600\text{Km/h}$. Then O-LAZ size need to satisfy $Z \geq 5$, $F_r \geq 0.2$ (Detailed calculations are given in Section V).

B. O-LAZ Sequence Design Based on ITROX

In this subsection, we propose a new algorithm, OA-ITROX, based on the original ITROX algorithm [40]. New O-LAZ sequences are obtained by minimizing the ISL metric, defined in (25). The optimization problem can be written as follows:

$$\arg \min_{\mathbf{a}} \text{ISL}_{\widetilde{AF}}(\mathbf{a}; Z \times F_r), \quad (28)$$

$$\text{subject to } |a_k| = 1, k = 0, 1, \dots, N-1.$$

Since (25) contains an integral operation, it is challenging to directly optimize $\text{ISL}_{\widetilde{AF}}(\mathbf{a}; Z \times F_r)$. Since $\widetilde{AF}_{\mathbf{a}}(\tau, f)$ can be well approximated when f is very small, we can verify that (28) is equivalent to the following simpler problem:

$$\arg \min_{\mathbf{a}} \sum_{\substack{\tau=-Z \\ \tau \neq 0}}^Z f_{\delta} \sum_{f \in \mathcal{F}} |\widetilde{AF}_{\mathbf{a}}(\tau, f)|^2, \quad (29)$$

$$\text{subject to } |a_k| = 1, k = 0, 1, \dots, N-1,$$

where $\mathcal{F} = \{0, \pm f_{\delta}, \pm 2f_{\delta}, \dots, \pm F_r\}$ (Without loss of generality, we can assume that F_r is a multiple of f_{δ} and $F_r = (M-1)f_{\delta}$).

Before introducing the OA-ITROX algorithm, let us represent the O-PAAF of sequences using matrices. We first define the periodic diagonal elements. The elements of the k -th periodic diagonal of matrix \mathbf{A} are given by

$$\text{diag}(\mathbf{A}, k) = [[\mathbf{A}]_{0,k}, \dots, [\mathbf{A}]_{i, [k+i]_N}, \dots, [\mathbf{A}]_{N-1, k-1}]^T,$$

where $k = 0, 1, \dots, N-1$. For example, let \mathbf{A} be a matrix of size 4×4 . Then we have

$$\begin{aligned} \text{diag}(\mathbf{A}, 0) &= [A_{0,0}, A_{1,1}, A_{2,2}, A_{3,3}]^T, \\ \text{diag}(\mathbf{A}, 1) &= [A_{0,1}, A_{1,2}, A_{2,3}, A_{3,0}]^T, \\ \text{diag}(\mathbf{A}, 2) &= [A_{0,2}, A_{1,3}, A_{2,0}, A_{3,1}]^T, \\ \text{diag}(\mathbf{A}, 3) &= [A_{0,3}, A_{1,0}, A_{2,1}, A_{3,2}]^T. \end{aligned}$$

Let $\text{DS}(\mathbf{A}, k)$ represents the sum of all the elements of the k -th periodic diagonal of matrix \mathbf{A} , i.e.,

$$\text{DS}(\mathbf{A}, k) = \sum \text{diag}(\mathbf{A}, k). \quad (30)$$

By (30), we can calculate the O-PAAF magnitudes by the following equation:

$$|\widetilde{AF}_{\mathbf{a}}(\tau, f)| = \begin{cases} |\text{DS}((\mathbf{a} \odot \mathbf{f})^{\mathbf{H}}, \tau)|, & f \geq 0; \\ |\text{DS}(\mathbf{a}(\mathbf{a} \odot \mathbf{f})^{\mathbf{H}}, N - \tau)|, & f < 0, \end{cases} \quad (31)$$

where $\mathbf{f} = [1, \zeta_N^f, \dots, \zeta_N^{f(N-1)}]^T$, $\tau = 0, 1, \dots, N-1$, and $f \in \mathbb{R}$.

Furthermore, we can obtain the complete matrix representation of the O-PAAF of sequences in (32), where $\mathbf{f}_m = [1, \zeta_N^{mf_{\delta}}, \dots, \zeta_N^{mf_{\delta}(N-1)}]^T$, $m = 0, 1, \dots, M-1$, $\mathbf{A}_{0,0} = \mathbf{a}\mathbf{a}^{\mathbf{H}}$ and $\mathbf{A}_{i,j} = (\mathbf{a} \odot \mathbf{f}_i)(\mathbf{a} \odot \mathbf{f}_j)^{\mathbf{H}}$.

$$\begin{aligned} & \begin{bmatrix} \mathbf{a} \\ \mathbf{a} \odot \mathbf{f}_1 \\ \vdots \\ \mathbf{a} \odot \mathbf{f}_{M-1} \end{bmatrix} \begin{bmatrix} \mathbf{a}^{\mathbf{H}} & (\mathbf{a} \odot \mathbf{f}_1)^{\mathbf{H}} & \cdots & (\mathbf{a} \odot \mathbf{f}_{M-1})^{\mathbf{H}} \end{bmatrix} \\ &= \begin{bmatrix} \mathbf{A}_{0,0} & \mathbf{A}_{0,1} & \cdots & \mathbf{A}_{0,M-1} \\ \mathbf{A}_{1,0} & \mathbf{A}_{1,1} & \cdots & \mathbf{A}_{1,M-1} \\ \vdots & \vdots & \ddots & \vdots \\ \mathbf{A}_{M-1,0} & \mathbf{A}_{M-1,1} & \cdots & \mathbf{A}_{M-1,M-1} \end{bmatrix}. \end{aligned} \quad (32)$$

According to (31), the O-PAAF matrix representation can be divided into three case.

Case I: $|\widetilde{AF}_{\mathbf{a}}(\tau, 0)| = |\text{DS}(\mathbf{A}_{0,0}, \tau)|$;

Case II: $|\widetilde{AF}_{\mathbf{a}}(\tau, mf_{\delta})| = |\text{DS}(\mathbf{A}_{m,0}, \tau)|$;

Case III: $|\widetilde{AF}_{\mathbf{a}}(\tau, -mf_{\delta})| = |\text{DS}(\mathbf{A}_{0,m}, N - \tau)|$.

Let

$$\Lambda = \{\mathbf{X} | \mathbf{X} = \mathbf{x}\mathbf{y}^{\mathbf{H}}\}, \quad (33)$$

where both \mathbf{x}, \mathbf{y} are unimodular sequences of length MN . In OA-ITROX algorithm, \mathbf{X} is always generated by the unimodular sequence \mathbf{a} which is being optimized, so it is commonly denoted as $\mathbf{X}_{\mathbf{a}}$. $\mathbf{X}_{\mathbf{a}}$ is given by

$$\mathbf{X}_{\mathbf{a}} = \mathbf{x}_{\mathbf{a}}\mathbf{y}_{\mathbf{a}}^{\mathbf{H}}, \quad (34)$$

where

$$\mathbf{x}_{\mathbf{a}} = \begin{bmatrix} \mathbf{a} \\ \mathbf{a} \odot \mathbf{f}_1 \\ \vdots \\ \mathbf{a} \odot \mathbf{f}_{M-1} \end{bmatrix}, \mathbf{y}_{\mathbf{a}} = \begin{bmatrix} \mathbf{a} \\ \mathbf{a} \odot \mathbf{f}_1 \\ \vdots \\ \mathbf{a} \odot \mathbf{f}_{M-1} \end{bmatrix}.$$

Also, let

$$\Gamma_Z = \left\{ \mathbf{Y} | \mathbf{Y} = \begin{bmatrix} \mathbf{Y}_{0,0} & \cdots & \mathbf{Y}_{0,M-1} \\ \vdots & & \vdots \\ \mathbf{Y}_{M-1,0} & \cdots & \mathbf{Y}_{M-1,M-1} \end{bmatrix} \right\}, \quad (35)$$

where \mathbf{Y} is a matrix of size $MN \times MN$, containing block matrices $\mathbf{Y}_{m,n}$ each of size $N \times N$, where $\mathbf{Y}_{0,0}$ satisfies

$$\text{DS}(\mathbf{Y}_{0,0}, \tau) = \begin{cases} N, & \tau = 0; \\ 0, & \tau = 1, \dots, Z, N-Z, \dots, N-1, \end{cases}$$

$\mathbf{Y}_{m,0}, \mathbf{Y}_{0,m}$ satisfy

$$\begin{aligned} \text{DS}(\mathbf{Y}_{m,0}, \tau) &= \text{DS}(\mathbf{Y}_{0,m}, N - \tau) \\ &= \begin{cases} \sum_{n=0}^{N-1} \zeta_N^{mf_{\delta}n}, & \tau = 0; \\ 0, & \tau = 1, \dots, Z, N-Z, \dots, N-1. \end{cases} \end{aligned}$$

The proposed OA-ITROX is a cyclic iterative algorithm that constantly finds the optimal projection (for the matrix Frobenius norm) between Λ and Γ_Z . In the following theorem, we study the orthogonal projection of an element of Λ on Γ_Z . This process can be described as follows:

$$\begin{aligned} & \arg \min_{\mathbf{Y}} \|\mathbf{Y} - \mathbf{X}\|_F^2, \\ & \text{s.t. } \mathbf{Y} \in \Gamma_Z. \end{aligned} \quad (36)$$

Theorem 1: Let $\mathbf{Y} = \mathbf{X}^{\perp}$ be the optimal projection of $\mathbf{X} \in \Lambda$ on Γ_Z , then \mathbf{Y} can be constructed through the following cases:

Case I: For $\tau = 0, Z+1, Z+2, \dots, N-1-Z$,

$$\text{diag}(\mathbf{Y}_{m,0}, \tau) = \text{diag}(\mathbf{X}_{m,0}, \tau),$$

$$\text{diag}(\mathbf{Y}_{0,m}, \tau) = \text{diag}(\mathbf{X}_{0,m}, \tau),$$

where $m = 0, 1, \dots, M-1$.

Case II: For $\tau = 1, \dots, Z, N-Z, \dots, N-1$,

$$\text{diag}(\mathbf{Y}_{m,0}, \tau) = \text{diag}(\mathbf{X}_{m,0}, \tau) - \frac{1}{N} \text{DS}(\mathbf{X}_{m,0}, \tau),$$

$$\text{diag}(\mathbf{Y}_{0,m}, \tau) = \text{diag}(\mathbf{X}_{0,m}, \tau) - \frac{1}{N} \text{DS}(\mathbf{X}_{0,m}, \tau),$$

where $m = 0, 1, \dots, M-1$.

Case III: For $m \neq 0$ or $n \neq 0$,

$$\mathbf{Y}_{m,n} = \mathbf{X}_{m,n},$$

where $\mathbf{X}_{m,n} = (\mathbf{a} \odot \mathbf{f}_m)(\mathbf{a} \otimes \mathbf{f}_n)^H$, $m, n = 0, 1, \dots, M-1$.

Proof: We have

$$\begin{aligned} \|\mathbf{Y} - \mathbf{X}\|_F^2 &= \sum_{\tau \neq 0} \sum_{m=0}^{M-1} (\|\text{diag}(\mathbf{Y}_{m,0}, \tau) - \text{diag}(\mathbf{X}_{m,0}, \tau)\|^2 \\ &\quad + \|\text{diag}(\mathbf{Y}_{0,m}, \tau) - \text{diag}(\mathbf{X}_{0,m}, \tau)\|^2). \end{aligned}$$

Our goal is to minimize $\|\mathbf{Y} - \mathbf{X}\|_F^2$ for $\mathbf{Y} \in \Gamma_Z$. Hence, we can minimize $g_{m,\tau}^{\text{col}}(\mathbf{Y}) := \|\text{diag}(\mathbf{Y}_{m,0}, \tau) - \text{diag}(\mathbf{X}_{m,0}, \tau)\|^2$ and $g_{m,\tau}^{\text{row}}(\mathbf{Y}) := \|\text{diag}(\mathbf{Y}_{0,m}, \tau) - \text{diag}(\mathbf{X}_{0,m}, \tau)\|^2$ for all $m = 0, 1, \dots, M-1$, $\tau = 1, \dots, Z, N-Z, \dots, N-1$. Denote $x_k^{(m,0,\tau)} = [\text{diag}(\mathbf{X}_{m,0}, \tau)]_k$ and $y_k^{(m,0,\tau)} = [\text{diag}(\mathbf{Y}_{m,0}, \tau)]_k$, where $k = 0, 1, \dots, N-1$. Then

$$g_{m,\tau}^{\text{col}}(\mathbf{Y}) = \sum_{k=0}^{N-1} |y_k^{(m,0,\tau)} - x_k^{(m,0,\tau)}|^2,$$

such that $\sum_{k=0}^{N-1} y_k^{(m,0,\tau)} = 0$. Using the Cauchy-Schwarz inequality we have that

$$g_{m,\tau}^{\text{col}}(\mathbf{Y}) \geq \frac{1}{N} \left| \sum_{k=0}^{N-1} \left(y_k^{(m,0,\tau)} - x_k^{(m,0,\tau)} \right) \right|^2.$$

Note that the equality holds if and only if $y_k^{(m,0,\tau)} = x_k^{(m,0,\tau)} - \frac{1}{N} \sum_{k=0}^{N-1} x_k^{(m,0,\tau)}$. Returning to the matrix representation, we can infer that the minimum value of $g_{m,\tau}^{\text{col}}(\mathbf{Y})$ is achieved at the point

$$\text{diag}(\mathbf{Y}_{m,0}, \tau) = \text{diag}(\mathbf{X}_{m,0}, \tau) - \frac{1}{N} \text{DS}(\mathbf{X}_{m,0}, \tau).$$

Similarly, we can prove that the minimum value of $g_{m,\tau}^{\text{row}}(\mathbf{Y})$ is achieved when

$$\text{diag}(\mathbf{Y}_{0,m}, \tau) = \text{diag}(\mathbf{X}_{0,m}, \tau) - \frac{1}{N} \text{DS}(\mathbf{X}_{0,m}, \tau).$$

In the next theorem, we find the optimal projection of $\mathbf{Y} \in \Gamma_Z$ in Λ , described as follows:

$$\begin{aligned} \arg \min_{\mathbf{X}} \|\mathbf{X} - \mathbf{Y}\|_F^2, \\ \text{s.t. } \mathbf{X} \in \Lambda. \end{aligned} \quad (37)$$

Theorem 2: Let $\mathbf{X} = \mathbf{Y}^\perp$ be the optimal projection of $\mathbf{Y} \in \Gamma_Z$ on Λ . Suppose \mathbf{Y} has the singular value decomposition (SVD)

$$\mathbf{S}\mathbf{\Sigma}\mathbf{V}^H = \mathbf{Y}, \quad (38)$$

then \mathbf{X} is given by

$$\mathbf{X} = M\mathbf{N}\mathbf{s}\mathbf{v}^H, \quad (39)$$

where \mathbf{s}, \mathbf{v} are the left and right singular vector corresponding to the largest singular value of \mathbf{Y} , respectively.

Proof: The proof is omitted, as it is similar to the proof of the optimal rank-1 matrix approximation given in [40]. ■

Note that we cannot construct \mathbf{a} from \mathbf{X} in *Theorem 2*. Hence, the process of generating sequence \mathbf{a} from matrix \mathbf{X} is described through the following optimization problem.

$$\begin{aligned} \arg \min_{\mathbf{a}} \|\mathbf{X}_{\mathbf{a}} - \mathbf{X}\|_F^2, \\ \text{s.t. } \mathbf{X}_{\mathbf{a}} = \mathbf{x}_{\mathbf{a}}\mathbf{y}_{\mathbf{a}}^H, \\ \mathbf{X} = M\mathbf{N}\mathbf{s}\mathbf{v}^H. \end{aligned} \quad (40)$$

It is equivalent to solving the following optimization problem:

$$\arg \min_{\mathbf{a}} \|\mathbf{x}_{\mathbf{a}} - \sqrt{MN}\mathbf{s}\|_F^2 + \|\mathbf{y}_{\mathbf{a}} - \sqrt{MN}\mathbf{v}\|_F^2. \quad (41)$$

Theorem 3: The problem (41) has a closed-form solution, which is given by

$$\begin{aligned} a[k] = \exp \left\{ i\varphi \left(\frac{1}{M} \sum_{m=0}^{M-1} \sqrt{MN} s[k+mM] / \zeta_N^{mf_\delta k} \right. \right. \\ \left. \left. + \frac{1}{M} \sum_{m=0}^{M-1} \sqrt{MN} v[k+mM] \cdot \zeta_N^{mf_\delta k} \right) \right\}, \end{aligned}$$

where $i = \sqrt{-1}$ is the imaginary unit, $k = 0, 1, \dots, N-1$.

Proof: The proof is omitted, as it is similar to the proof of the optimal approximation in the AF-CAO algorithm [34]. ■

The proposed OA-ITROX for the local minimization of the ISL metric in (29) can be summarized in **Algorithm 1**.

Algorithm 1: The OA-ITROX algorithm

Input: Sequence length N ; O-LAZ size $Z \times F_r$; Maximum iterations number MaxIterNum ; Initial point \mathbf{a}^0 is a random sequence. Let $t = 1$.

Step 1: Calculate $\mathbf{X}_{\mathbf{a}}^{t-1} = (\mathbf{x}_{\mathbf{a}}^{t-1})(\mathbf{y}_{\mathbf{a}}^{t-1})^H$ and find $\mathbf{Y}^t \in \Gamma_Z$ according to *Theorem 1*.

Step 2: Compute the SVD of \mathbf{Y}^t and find $\mathbf{X}^t \in \Lambda$ according to *Theorem 2*.

Step 3: Let the left-singular vector and right-singular vector of corresponding to the maximum singular value of \mathbf{X}^t be \mathbf{s}, \mathbf{v} , respectively. Then the unimodular sequences \mathbf{a}^t is obtained by *Theorem 3*.

Iteration: Repeat Steps 1-3 until some stop criterion is satisfied, e.g., $\|\mathbf{a}^t - \mathbf{a}^{t-1}\|^2 \leq \varepsilon$, where ε is a predefined threshold, or $t \leq \text{MaxIterNum}$. Otherwise, update $t = t + 1$ and continue the iterations.

Output: Set the optimized sequence as \mathbf{a} .

Remark 4: In the proposed OA-IROTX algorithm, the choice of the parameter f_δ is important. From the principles of Riemann integrals in mathematical analysis [69], it can be observed that if f_δ is too large, (29) cannot closely approximate (28). However, if f_δ is too small, the complexity of the algorithm will increase significantly. Taking into account the two reasons mentioned above, we suggest setting the value of f_δ between 0.1 and 0.2. If the parameter f_δ is set to 1, then the objective function reduces to the traditional AF $AF_{\mathbf{a}}(\tau, f)$.

Remark 5: The primary computational cost of **Algorithm 1** comes from Step 2. Therefore, the complexity of **Algorithm 1** is determined by the complexity of SVD decomposition. In general, for matrix A of size $m \times n$, the complexity of SVD is $\mathcal{O}(mn \times \min(m, n))$ [70]. Since we are concerned with the maximum singular value only, we can employ power method to reduce the complexity from $\mathcal{O}(mn \times \min(m, n))$ to $\mathcal{O}(mn)$

[70]. Hence, in this work, the complexity of OA-ITROX is $\mathcal{O}\left(\left(\frac{NF_r}{f_\delta}\right)^2\right)$.

Remark 6: ITROX outperforms some other algorithms from the following perspectives:

- AF-CAO requires the correlation matrix to be a block diagonal matrix.
- AISO requires the first majorization function to be a real-valued function.
- GD has excessively high algorithmic complexity and hence is not suitable for constructing O-LAZ sequences.

V. NUMERICAL EXPERIMENTS

A. Performance Analysis of OA-ITROX Algorithm

Using the proposed algorithm, we have designed an unimodular sequence of length $N = 128$ with low O-AF zone $(Z \times F_r) = (32 \times 0.2)$. The OA-ITROX algorithm is initialized with random phase sequence. The maximum iteration number is set to 2×10^6 and $f_\delta = 0.2$.

To provide a clear description of the performance of OA-ITROX algorithm within the O-LAZ, we define the ambiguity level (dB) as follows

$$\text{ambiguity level} = 20 \log_{10} \frac{|\widetilde{AF}_{\mathbf{a}}(\tau, f)|}{|\widetilde{AF}_{\mathbf{a}}(0, 0)|}.$$

The planform figure of the O-AF of the generated sequence is shown in Fig. 2. The the O-LAZ is highlighted with a red solid line box. It can be observed that within the O-LAZ, the ambiguity level of O-AF is consistently below -40 dB.

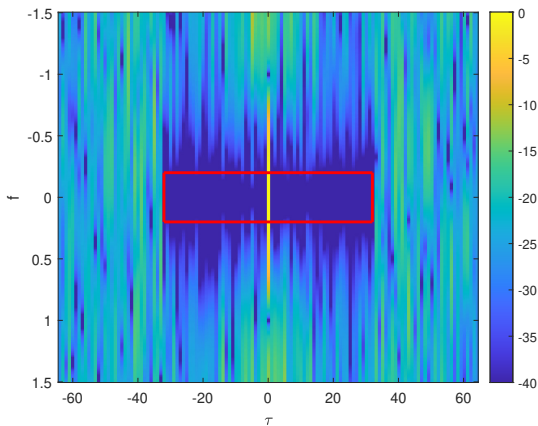


Fig. 2. The planform figure of the O-AF of the o-LAZ sequence generated by OA-ITROX algorithm.

Fig. 3 shows the ISL value of the objective function with the number of iterations during the execution of the OA-ITROX algorithm. In this experiment, the sequence lengths and O-LAZ size are set as $N = 64, 128, 256, 512, 1024$, $Z = N/4, F_r = 0.2$. This indicates that the proposed modified ITROX algorithm has good convergence in every sequence length.

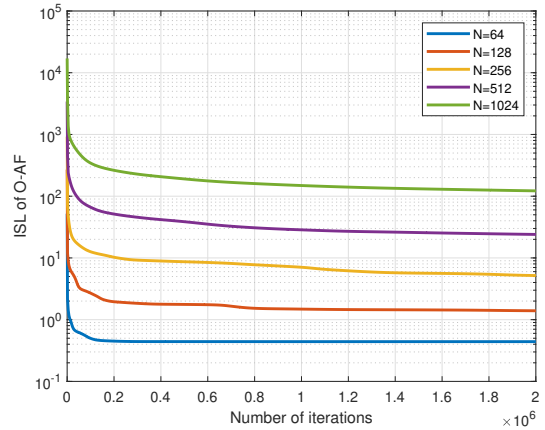


Fig. 3. Semi-log plot of the ISL with respect to the iteration index.

B. Performance Comparison with Traditional AF

As mentioned in *Remark 3*, if we set $f_\delta = 1$, OA-ITROX can optimize the traditional AF which leads to traditional LAZ sequences. In this section, we evaluate the performances of the traditional LAZ sequences constructed using the proposed OA-ITROX algorithm and the AF-CAO algorithm [22], [34] when optimizing the traditional AF.

We consider the sequence length of $N = 128$, the LAZ size of $(Z \times F_r) = (8 \times 4)$, the maximum iteration number of 3×10^6 , and a random sequence as the initial solution. Fig. 4 shows the planform figure of the traditional LAZ sequence constructed using AF-CAO algorithm and OA-ITROX, respectively. Fig. 5 provides a comparison of ISL changes with the number of iterations. Fig. 4 and Fig. 5 show that OA-ITROX algorithm can be employed to design sequences having good traditional AF magnitudes. Furthermore, OA-ITROX outperforms the AF-CAO algorithm in terms of AF sidelobe. Within the LAZ, sequences generated by the AF-CAO algorithm exhibit uneven sidelobes, with higher values around the four corners. In contrast, sequences generated by the OA-ITROX algorithm demonstrate uniform sidelobes within the LAZ, all about -50 dB.

C. Simulation Results

We assume the number of subcarriers $N = 128$, cyclic prefix (CP) length $N_{CP} = 32$, the IF frequency $f_c = 3.4$ GHz, the interval of subcarriers $\Delta f = 15$ KHz, maximum relative speed $v_{max} = 500$ Km/h. In addition, we set the power delay profile according to the EVA channel parameters defined in the 3GPP standards [6]. From [71], the maximum Doppler frequency f_d is calculated as $v f_c / c = 1.57$ KHz. Consequently, the normalized Doppler frequency is 0.105.

We have designed two simulation experiments. The first simulation experiment focuses on the channel estimation performance of a single OFDM pilot symbol. As described in Subsection II-B, a single OFDM pilot symbol provides an estimate $\hat{\mathbf{h}}$ of the channel response \mathbf{h}_{mid} . Therefore, the MSE of the midpoint instant is defined as follows:

$$\text{MSE}_{mid} = E \left(\|\mathbf{h}_{mid} - \hat{\mathbf{h}}\|_2^2 \right).$$

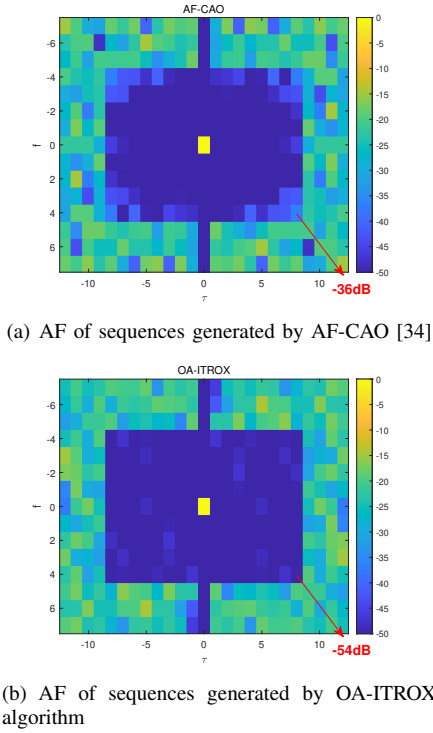


Fig. 4. The planform figure of the traditional AF of the sequences.

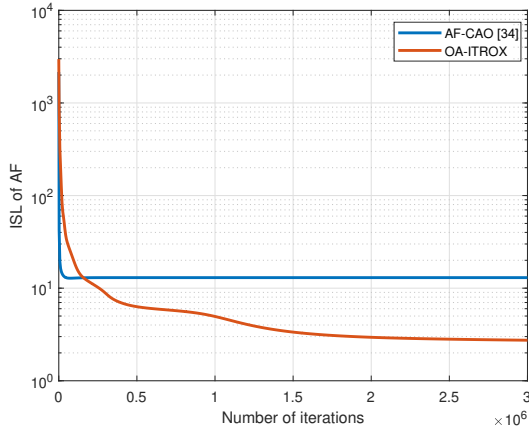


Fig. 5. Semi-log plot of the ISL with respect to the iteration index.

For benchmarking, we select the following three sequences as pilot sequences and conduct channel estimation simulation experiments. The first sequence is a Zadoff-Chu (ZC) sequence of length $N = 128$, which is given by

$$\mathbf{s}_{zc}^{(\mu)} = [s_{zc}^{(\mu)}[0], s_{zc}^{(\mu)}[1], \dots, s_{zc}^{(\mu)}[127]]^T,$$

where $s_{zc}^{(\mu)}[k] = \zeta_{2N}^{-\mu k^2}$ and $\gcd(\mu, N) = 1$. The second sequence is an extended m -sequence of length $N = 128$, which is given by

$$\mathbf{s}_m = [s_m[0], s_m[1], \dots, s_m[126], 1]^T,$$

where $s_m[k] = (-1)^{\text{Tr}(\alpha^k)}$, α is the primitive element of Galois field $GF(2, 7)$, and $\text{Tr}(\cdot)$ is the Trace function over $GF(2, 7)$. The third sequence is a traditional LAZ sequence,

which is generated by AF-CAO algorithm [34]. We set the parameters for AF-CAO algorithm are as follows: $N = 128$, $Z = 32$, $F_r = 1$ and maximum iteration number 2×10^6 . Note that, since it does not consider the impact of O-AF, this sequence may serve as a baseline to measure the effective gain of O-LAZ sequences. The fourth sequence is O-LAZ sequence which is constructed using the proposed OA-ITROX algorithm. The input parameters for the algorithm are as follows: $N = 128$, $Z = 32$, $F_r = f_\delta = 0.2$ and maximum iteration number 2×10^6 .

Remark 7: ZC sequences and m sequences are not unique. Here, we calculated the ISL of O-AF for 64 ZC sequences and 18 m -sequences with parameters $Z = 32$, $F_r = 0.2$. We have chosen the sequences with the highest and lowest ISL magnitude, and denoted them as “The best ZC/ m -sequence” and “The worst ZC/ m -sequence,” respectively. Furthermore, the best ZC sequence is used as the initial seed sequence for the OA-ITROX algorithm, to construct the O-LAZ sequence.

Fig. 6 shows the MSE of the midpoint instant from five pilots. The dashed line “CRLB” in Fig. 6 represents the Cramer-Rao Lower Bound (CRLB) under time-invariant conditions, where $\text{CRLB} = \frac{N_{\text{CP}}}{N} \sigma^2$ [31], [72], [73]. From Fig. 6, the O-LAZ sequence outperforms the other four sequences significantly with respect to channel estimation performance. From Fig. 6, the proposed O-LAZ sequence exhibits about a 6 dB gain compared to the best ZC sequence. Moreover, the estimation performance of the O-LAZ sequence is very close to the CRLB when the SNR is below 20 dB. This indicates that the O-LAZ sequence can effectively suppress the ICI interference caused by DSC, thereby achieving channel estimation performance close to that of a time-invariant channel.

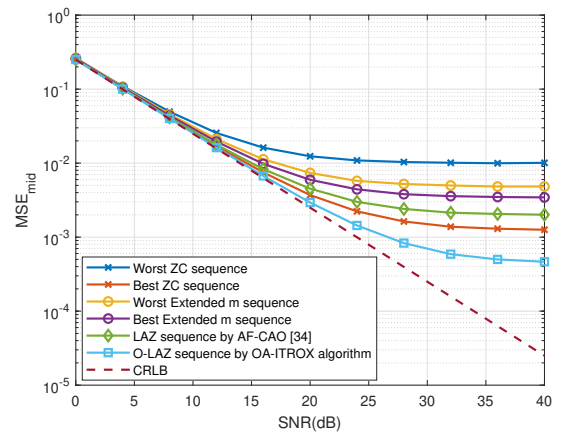


Fig. 6. The MSE of the midpoint instant from six pilots.

The second simulation experiment considers channel estimation performance and bit error rate (BER) performance for multiple OFDM symbols. Here, we adopt the transmission frame structure as shown in Fig. 1 and use DPSS interpolation to get the channel state information of data symbols. The detailed process of DPSS interpolation is provided in Appendix II. We assume a total of $M_P = 8$ pilot symbols, with each pair of pilot OFDM symbols containing $M_D = 1$ data OFDM symbols. All other simulation parameters remain

the same as in the previous experiment. In this experiment, the parameters for generating DPSS interpolation are as follows: The number of DPSS is 8, and the time half bandwidth is 2.02. As described in Subsection II.C, there are a total of $M = M_P + M_D(M_P - 1)$ OFDM symbols. Hence, the time-domain channel matrix \mathbf{h} corresponding to the OFDM frame with CPs should be an $L \times (N + L)M$ matrix. And the $\text{MSE}_{\text{frame}}$ of the total OFDM frame is defined as follows:

$$\text{MSE}_{\text{frame}} = \frac{E \left(\|\mathbf{h} - \hat{\mathbf{h}}\|_F^2 \right)}{(N + L)M}.$$

Fig. 7 shows the MSE of the OFDM frame from three pilots. Although the DPSS interpolation process introduces new errors, the overall estimation performance remains quite satisfactory. The proposed O-LAZ sequence outperforms the best ZC sequence, extended m sequence, and traditional LAZ sequence, significantly in terms of channel estimation MSE. From Fig. 7, the O-LAZ sequence exhibits about a 3 dB gain compared to the best ZC sequence.

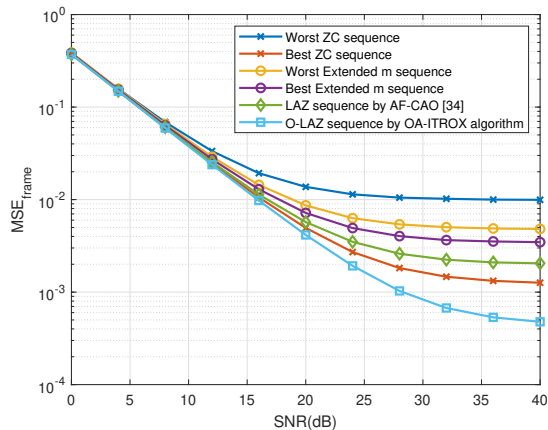


Fig. 7. The MSE of the OFDM frame from six pilots.

In Fig. 8, we employed quadrature phase shift keying (QPSK) as the modulation scheme for data symbols. Fig. 8 shows the BER performance of data symbols with various pilot sequences. The dashed lines represent the BER at the receiver with perfect knowledge of the channel state information (CSI). It is evident from Fig. 8 that the O-LAZ sequences outperform the best ZC sequence, extended m sequence, and traditional LAZ sequence, in terms of the BER performance. Moreover, the performance of the O-LAZ sequences closely approaches that of the dashed lines.

VI. CONCLUSION

In this paper, we have introduced O-AF and shown that sequences with low O-AF magnitude are suitable for performing channel estimation under DSC, without guard subcarriers, when the channel is approximated through Jakes' model of the Rayleigh fading channel. We have then proposed O-LAZ sequences using a modified ITROX algorithm. Finally, through numerical experiments we have demonstrated the robustness of the algorithm and efficiency of the designed O-LAZ sequences

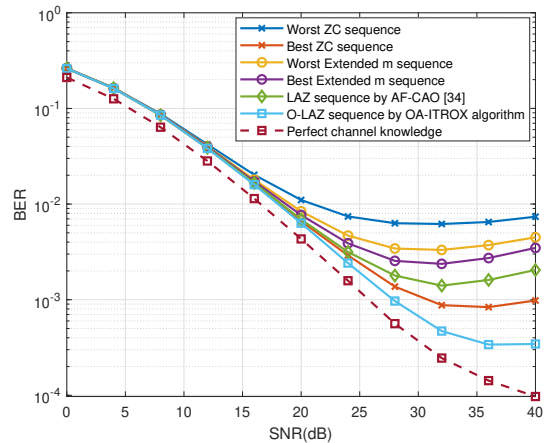


Fig. 8. The BER of the data symbols using different pilot sequences.

for efficient channel estimation under DSC as compared to the traditional ZC and m sequences.

ACKNOWLEDGMENT

The authors are very grateful to the associate editor, Prof. Sajid Ahmed, and the anonymous reviewers for their valuable comments and suggestions that greatly improved the presentation and quality of this article.

REFERENCES

- [1] J. Wu and P. Fan, "A survey on high mobility wireless communications: Challenges, opportunities and solutions," *IEEE Access*, vol. 4, pp. 450–476, 2016.
- [2] X. Ma, G. B. Giannakis, and S. Ohno, "Optimal training for block transmissions over doubly selective wireless fading channels," *IEEE Trans. Signal Process.*, vol. 51, no. 5, pp. 1351–1366, 2003.
- [3] G. Leus, "On the estimation of rapidly time-varying channels," in *Proc. IEEE Eur. Signal Process. Conf.*, 2004, pp. 2227–2230.
- [4] F. Qu and L. Yang, "On the estimation of doubly-selective fading channels," *IEEE Trans. Wireless Commun.*, vol. 9, no. 4, pp. 1261–1265, 2010.
- [5] M. Noor-A-Rahim, Z. Liu, H. Lee, M. O. Khyam, J. He, D. Pesch, K. Moessner, W. Saad, and H. V. Poor, "6G for vehicle-to-everything (V2X) communications: Enabling technologies, challenges, and opportunities," *Proceedings of the IEEE*, vol. 110, no. 6, pp. 712–734, 2022.
- [6] 3GPP, "3GPP TR 38.811 - Study on New Radio (NR) to support non-terrestrial networks," *V15. 4.0*, 2020.
- [7] Y. S. Cho, J. Kim, W. Y. Yang, and C. G. Kang, *MIMO-OFDM wireless communications with MATLAB*. John Wiley & Sons, 2010.
- [8] A. Kannu and P. Schniter, "Mse-optimal training for linear time-varying channels," in *Proceedings.(ICASSP'05). IEEE International Conference on Acoustics, Speech, and Signal Processing, 2005.*, vol. 3. IEEE, 2005, pp. iii–789.
- [9] J. K. Tugnait and W. Luo, "Linear prediction error method for blind identification of periodically time-varying channels," *IEEE Transactions on Signal Processing*, vol. 50, no. 12, pp. 3070–3082, 2002.
- [10] Z. Tang, R. C. Cannizzaro, G. Leus, and P. Banelli, "Pilot-assisted time-varying channel estimation for OFDM systems," *IEEE Trans. Signal Process.*, vol. 55, no. 5, pp. 2226–2238, 2007.
- [11] K. Z. Islam, T. Y. Al-Naffouri, and N. Al-Dhahir, "On optimum pilot design for Comb-type OFDM transmission over doubly-selective channels," *IEEE Trans. Commun.*, vol. 59, no. 4, pp. 930–935, 2011.
- [12] J. K. Tugnait, S. He, and H. Kim, "Doubly selective channel estimation using exponential basis models and subblock tracking," *IEEE Transactions on Signal Processing*, vol. 58, no. 3, pp. 1275–1289, 2009.
- [13] R. Chopra and C. R. Murthy, "Data aided MSE-optimal time varying channel tracking in massive MIMO systems," *IEEE Transactions on Signal Processing*, vol. 69, pp. 4219–4233, 2021.

- [14] Y. Liao, G. Sun, Z. Cai, X. Shen, and Z. Huang, "Nonlinear Kalman filter-based robust channel estimation for high mobility OFDM systems," *IEEE Transactions on Intelligent Transportation Systems*, vol. 22, no. 11, pp. 7219–7231, 2020.
- [15] A. Mohebbi, H. Abdzadeh-Ziabari, W.-P. Zhu, and M. O. Ahmad, "Doubly selective channel estimation algorithms for millimeter wave hybrid MIMO systems," *IEEE Transactions on Vehicular Technology*, vol. 70, no. 12, pp. 12 821–12 835, 2021.
- [16] D. Chu, "Polyphase codes with good periodic correlation properties (corresp.)," *IEEE Trans. Inf. Theory*, vol. 18, no. 4, pp. 531–532, 1972.
- [17] P. Fan and M. Darnell, *Sequence design for communications applications*. Research Studies Press, 1996.
- [18] S. W. Golomb and G. Gong, *Signal design for good correlation: for wireless communication, cryptography, and radar*. Cambridge University Press, 2005.
- [19] P. Z. Fan, N. Suehiro, N. Kuroyanagi, and X. M. Deng, "Class of binary sequences with zero correlation zone," *Electron. Lett.*, vol. 35, no. 10, pp. 777–779, 1999.
- [20] X. H. Tang, P. Z. Fan, and S. Matsufuji, "Lower bounds on correlation of spreading sequence set with low or zero correlation zone," *Electron. Lett.*, vol. 36, no. 6, p. 1, 2000.
- [21] N. Levanon and E. Mozeson, *Radar signals*. New York, NY, USA: Wiley, 2004.
- [22] H. He, J. Li, and P. Stoica, *Waveform design for active sensing systems: a computational approach*. Cambridge University Press, 2012.
- [23] Z. Ye, Z. Zhou, P. Fan, Z. Liu, X. Lei, and X. Tang, "Low ambiguity zone: Theoretical bounds and Doppler-resilient sequence design in integrated sensing and communication systems," *IEEE J. Sel. Area. Comm.*, vol. 40, no. 6, pp. 1809–1822, 2022.
- [24] X. Deng and P. Fan, "Spreading sequence sets with zero correlation zone," *Electron. Lett.*, vol. 36, no. 11, p. 1, 2000.
- [25] A. R. Adhikary, Z. Zhou, Y. Yang, and P. Fan, "Constructions of cross z-complementary pairs with new lengths," *IEEE Trans. Signal Process.*, vol. 68, pp. 4700–4712, 2020.
- [26] Z. Gu, Z. Zhou, A. R. Adhikary, Y. Feng, and P. Fan, "Asymptotically optimal Golay-ZCZ sequence sets with flexible length," *Chinese J. Electron.*, vol. 32, no. 4, pp. 806–820, 2023.
- [27] X. Tang and W. H. Mow, "A new systematic construction of zero correlation zone sequences based on interleaved perfect sequences," *IEEE Trans. Inf. Theory*, vol. 54, no. 12, pp. 5729–5734, 2008.
- [28] X. Tang, P. Fan, and J. Lindner, "Multiple binary ZCZ sequence sets with good cross-correlation property based on complementary sequence sets," *IEEE Trans. Inf. Theory*, vol. 56, no. 8, pp. 4038–4045, 2010.
- [29] K. Liu, Z. Zhou, A. R. Adhikary, and C. Tang, "Large sets of binary spreading sequences with low correlation and low papr via gold functions," *IEEE Trans. Inf. Theory*, vol. 70, no. 7, pp. 5309–5322, 2024.
- [30] A. R. Adhikary, Y. Feng, Z. Zhou, and P. Fan, "Asymptotically optimal and near-optimal aperiodic quasi-complementary sequence sets based on florentine rectangles," *IEEE Trans. Commun.*, vol. 70, no. 3, pp. 1475–1485, 2022.
- [31] Z. Gu, Z. Zhou, A. R. Adhikary, Y. Feng, and P. Fan, "Asymptotically optimal Golay-ZCZ sequence sets with flexible length," *Chinese J. Electron.*, vol. 32, no. 4, pp. 806–820, 2023.
- [32] G. Cui, A. De Maio, A. Farina, and J. Li, *Radar waveform design based on optimization theory*. SciTech Publishing, 2020.
- [33] H. Deng, "Polyphase code design for orthogonal netted radar systems," *IEEE Trans. Signal Process.*, vol. 52, no. 11, pp. 3126–3135, 2004.
- [34] J. Li, P. Stoica, and X. Zheng, "Signal synthesis and receiver design for MIMO radar imaging," *IEEE Trans. Signal Process.*, vol. 56, no. 8, pp. 3959–3968, 2008.
- [35] P. Stoica, H. He, and J. Li, "New algorithms for designing unimodular sequences with good correlation properties," *IEEE Trans. Signal Process.*, vol. 57, no. 4, pp. 1415–1425, 2009.
- [36] —, "On designing sequences with impulse-like periodic correlation," *IEEE Signal Process. Lett.*, vol. 16, no. 8, pp. 703–706, 2009.
- [37] J. Song, P. Babu, and D. P. Palomar, "Optimization methods for designing sequences with low autocorrelation sidelobes," *IEEE Trans. Signal Process.*, vol. 63, no. 15, pp. 3998–4009, 2015.
- [38] J. Nocedal and S. J. Wright, *Numerical optimization*. Springer, 1999.
- [39] Y.-C. Wang, L. Dong, X. Xue, and K.-C. Yi, "On the design of constant modulus sequences with low correlation sidelobe levels," *IEEE Commun. Lett.*, vol. 16, no. 4, pp. 462–465, 2012.
- [40] M. Soltanalian and P. Stoica, "Computational design of sequences with good correlation properties," *IEEE Trans. Signal Process.*, vol. 60, no. 5, pp. 2180–2193, 2012.
- [41] Z. Gu, A. R. Adhikary, Z. Zhou, and P. Fan, "A computational design of aperiodic mismatched filtering sequences," in *2022 IEEE International Symposium on Information Theory (ISIT)*. IEEE, 2022, pp. 2643–2647.
- [42] Z. Gu, A. R. Adhikary, Z. Zhou, and M. Yang, "A computational design of unimodular complementary and Z-complementary sets," in *2023 IEEE International Symposium on Information Theory (ISIT)*. IEEE, 2023, pp. 1419–1424.
- [43] H. Wu, Z. Song, H. Fan, and Q. Fu, "Designing sequence with low sidelobe levels at specified intervals based on PSD fitting," *Electron. Lett.*, vol. 51, no. 1, pp. 99–101, 2015.
- [44] J. M. Baden, B. O'Donnell, and L. Schmieder, "Multiobjective sequence design via gradient descent methods," *IEEE Trans. Aerosp. Electron. Syst.*, vol. 54, no. 3, pp. 1237–1252, 2017.
- [45] M. A. Kerahroodi, A. Aubry, A. De Maio, M. M. Naghsh, and M. Modarres-Hashemi, "A coordinate-descent framework to design low PSL/ISL sequences," *IEEE Trans. Signal Process.*, vol. 65, no. 22, pp. 5942–5956, 2017.
- [46] J. Wang and Y. Wang, "Designing unimodular sequences with optimized auto/cross-correlation properties via consensus-ADMM/PDMM approaches," *IEEE Trans. Signal Process.*, vol. 69, pp. 2987–2999, 2021.
- [47] O. Rezaei, M. Ahmadi, M. M. Naghsh, A. Aubry, M. M. Nayebi, and A. De Maio, "A learning-inspired strategy to design binary sequences with good correlation properties: SISO and MIMO radar systems," *IEEE Trans. Aerosp. Electron. Syst.*, 2023.
- [48] J. Liang, H. C. So, C. S. Leung, J. Li, and A. Farina, "Waveform design with unit modulus and spectral shape constraints via Lagrange programming neural network," *IEEE J. Sel. Top. Signal Process.*, vol. 9, no. 8, pp. 1377–1386, 2015.
- [49] L. Zhao, J. Song, P. Babu, and D. P. Palomar, "A unified framework for low autocorrelation sequence design via majorization-minimization," *IEEE Trans. Signal Process.*, vol. 65, no. 2, pp. 438–453, 2016.
- [50] H. Esmacili-Najafabadi, M. Ataei, and M. F. Sabahi, "Designing sequence with minimum PSL using Chebyshev distance and its application for chaotic MIMO radar waveform design," *IEEE Trans. Signal Process.*, vol. 65, no. 3, pp. 690–704, 2016.
- [51] Y. Li and S. A. Vorobyov, "Fast algorithms for designing unimodular waveform(s) with good correlation properties," *IEEE Trans. Signal Process.*, vol. 66, no. 5, pp. 1197–1212, 2017.
- [52] R. Lin, M. Soltanalian, B. Tang, and J. Li, "Efficient design of binary sequences with low autocorrelation sidelobes," *IEEE Trans. Signal Process.*, vol. 67, no. 24, pp. 6397–6410, 2019.
- [53] A. Aubry, A. De Maio, B. Jiang, and S. Zhang, "Ambiguity function shaping for cognitive radar via complex quartic optimization," *IEEE Trans. Signal Process.*, vol. 61, no. 22, pp. 5603–5619, 2013.
- [54] F. Arlery, R. Kassab, U. Tan, and F. Lehmann, "Efficient gradient method for locally optimizing the periodic/aperiodic ambiguity function," in *2016 IEEE Radar Conference (RadarConf)*. IEEE, 2016, pp. 1–6.
- [55] L. Wu, P. Babu, and D. P. Palomar, "Cognitive radar-based sequence design via SINR maximization," *IEEE Trans. Signal Process.*, vol. 65, no. 3, pp. 779–793, 2016.
- [56] G. Cui, Y. Fu, X. Yu, and J. Li, "Local ambiguity function shaping via unimodular sequence design," *IEEE Signal Process. Lett.*, vol. 24, no. 7, pp. 977–981, 2017.
- [57] Y. Fu, G. Cui, X. Yu, T. Zhang, L. Kong, and X. Yang, "Ambiguity function design via accelerated iterative sequential optimization," in *2017 IEEE Radar Conference (RadarConf)*. IEEE, 2017, pp. 0698–0702.
- [58] Y. Jing, J. Liang, B. Tang, and J. Li, "Designing unimodular sequence with low peak of sidelobe level of local ambiguity function," *IEEE Trans. Aerosp. Electron. Syst.*, vol. 55, no. 3, pp. 1393–1406, 2018.
- [59] K. Alhujaili, V. Monga, and M. Rangaswamy, "Quartic gradient descent for tractable radar slow-time ambiguity function shaping," *IEEE Trans. Aerosp. Electron. Syst.*, vol. 56, no. 2, pp. 1474–1489, 2019.
- [60] H. Esmacili-Najafabadi, H. Leung, and P. W. Moo, "Unimodular waveform design with desired ambiguity function for cognitive radar," *IEEE Trans. Aerosp. Electron. Syst.*, vol. 56, no. 3, pp. 2489–2496, 2019.
- [61] W. Wei and Y. Wei, "Unimodular sequence set design for MIMO radar ambiguity function shaping," in *2023 IEEE Radar Conference (RadarConf23)*. IEEE, 2023, pp. 1–5.
- [62] H. Hu, K. Zhong, C. Pan, and X. Xiao, "Ambiguity function shaping via manifold optimization embedding with momentum," *IEEE Commun. Lett.*, 2023.
- [63] J. Li and P. Stoica, *MIMO radar signal processing*. John Wiley & Sons, 2008.
- [64] T. Zemen and C. F. Mecklenbrauker, "Time-variant channel estimation using discrete prolate spheroidal sequences," *IEEE Trans. Signal Process.*, vol. 53, no. 9, pp. 3597–3607, 2005.

$$\arg \min_{\mathbf{a}} \int_{-F_r}^{F_r} \cdots \int_{-F_r}^{F_r} \left\| (\mathbf{A}_T^H \mathbf{A}_T)^{-1} \mathbf{A}_T^H (\mathbf{A}_T \odot \boldsymbol{\Omega}_q) - \text{diag}(\boldsymbol{\Gamma}_q) \right\|_F^2 d\omega_q^{(0)} \cdots d\omega_q^{(L-1)}. \quad (42)$$

$$\arg \min_{\mathbf{a}} \int_{-F_r}^{F_r} \cdots \int_{-F_r}^{F_r} \left\| \frac{1}{N} \mathbf{A}_T^H (\mathbf{A}_T \odot \boldsymbol{\Omega}_q) - \text{diag}(\boldsymbol{\Gamma}_q) \right\|_F^2 d\omega_q^{(0)} \cdots d\omega_q^{(L-1)}. \quad (43)$$

- [65] Y. Mostofi and D. C. Cox, "ICI mitigation for pilot-aided OFDM mobile systems," *IEEE Trans. Wireless Commun.*, vol. 4, no. 2, pp. 765–774, 2005.
- [66] Y. R. Zheng and C. Xiao, "Simulation models with correct statistical properties for Rayleigh fading channels," *IEEE Trans. Commun.*, vol. 51, no. 6, pp. 920–928, 2003.
- [67] S. M. Kay, *Fundamentals of statistical signal processing: estimation theory*. Prentice-Hall, Inc., 1993.
- [68] U. E. U. conformance specification Radio, "3rd generation partnership project; technical specification group radio access network; evolved universal terrestrial radio access (E-UTRA); user equipment (UE) conformance specification radio transmission and reception," *3GPP*, 2011.
- [69] V. A. Zorich, *Integration*. Berlin, Heidelberg: Springer Berlin Heidelberg, 2015, pp. 331–408. [Online]. Available: https://doi.org/10.1007/978-3-662-48792-1_6
- [70] G. H. Golub and C. F. Van Loan, *Matrix computations*. JHU press, 2013.
- [71] F. Hlawatsch and G. Matz, *Wireless communications over rapidly time-varying channels*. Academic press, 2011.
- [72] P. Spasojevic and C. N. Georghiades, "Complementary sequences for ISI channel estimation," *IEEE Transactions on Information Theory*, vol. 47, no. 3, pp. 1145–1152, 2001.
- [73] G. Gong, F. Huo, and Y. Yang, "Large zero autocorrelation zones of Golay sequences and their applications," *IEEE Transactions on Communications*, vol. 61, no. 9, pp. 3967–3979, 2013.
- [74] A.-M. Wazwaz, *Preliminaries*. Berlin, Heidelberg: Springer Berlin Heidelberg, 2011, pp. 3–31. [Online]. Available: https://doi.org/10.1007/978-3-642-21449-3_1

APPENDIX I

Note that (22) has two random variables $g_q^{(l)}$ and $\omega_q^{(l)}$. Out of the two random variables, the randomness of $\omega_q^{(l)}$ needs to be eliminated to ensure that the resultant sequence efficiently estimates the channel under any channel parameters. Hence, CR_2 is modified from (22) to (42). For efficient channel estimation over DSC, pilot sequences need to satisfy both (21) and (42). However, satisfying both (21) and (42) can be a challenging optimization problem. Hence, we re-design (21) and (42) using the ISL of the O-AF of sequence \mathbf{a} and combine CR_1 and CR_2 to a single optimization problem.

Note that minimizing (21) is equivalent to minimizing $|\widetilde{\text{AF}}_{\mathbf{a}}(\tau, 0)|$. Therefore, if we minimize the ISL, CR_1 will also be satisfied. Next, if $\mathbf{A}_T^H \mathbf{A}_T = N\mathbf{I}$, then (42) can be simplified to (43). For the ease of expression, we denote the integrand function in (43) as:

$$\eta_1(\omega_q^{(0)}, \dots, \omega_q^{(L-1)}) = \left\| \frac{1}{N} \mathbf{A}_T^H (\mathbf{A}_T \odot \boldsymbol{\Omega}_q) - \text{diag}(\boldsymbol{\Gamma}_q) \right\|_F^2. \quad (44)$$

And (43) can be rewritten as:

$$\arg \min_{\mathbf{a}} \int_{-F_r}^{F_r} \cdots \int_{-F_r}^{F_r} \eta_1(\omega_q^{(0)}, \dots, \omega_q^{(L-1)}) d\omega_q^{(0)} \cdots d\omega_q^{(L-1)}. \quad (45)$$

Expanding (44), we obtain (46).

According to the definition of O-AF, (46) can be approximated by (47).

Hence, (45) can be approximated as follows:

$$\arg \min_{\mathbf{a}} \int_{-F_r}^{F_r} \cdots \int_{-F_r}^{F_r} \eta_2(\omega_q^{(0)}, \dots, \omega_q^{(L-1)}) d\omega_q^{(0)} \cdots d\omega_q^{(L-1)}. \quad (48)$$

Since the values of $\omega_q^{(l)}$, for each $l = 0, \dots, L-1$ lies within $[-F_r, F_r]$, the minimization problem of the multiple integral in (48) can be approximated as the minimization problem of a single integral [74], as follows:

$$\arg \min_{\mathbf{a}} \int_{-F_r}^{F_r} \eta_3(f) df, \quad (49)$$

where the integrand $\eta_3(f)$ is given by (50).

The problem of minimizing (49) can be approximately replaced by the following minimization problem:

$$\arg \min_{\mathbf{a}} \int_{-F_r}^{F_r} \frac{1}{N} \left(\sum_{\substack{\tau=-Z \\ \tau \neq 0}}^Z |\widetilde{\text{AF}}_{\mathbf{a}}(\tau, f)|^2 \right) df. \quad (51)$$

By exchanging the order of integration and summation, we have

$$\arg \min_{\mathbf{a}} \frac{1}{N} \sum_{\substack{\tau=-Z \\ \tau \neq 0}}^Z \int_{-F_r}^{F_r} |\widetilde{\text{AF}}_{\mathbf{a}}(\tau, f)|^2 df. \quad (52)$$

APPENDIX II

We adopt the transmission frame structure as shown in Fig. 2. It is assumed that the midpoint instant channel response of the pilot symbols is obtained by (9). Let $\mathbf{h}_{\text{frame}}$ denotes the channel response of the M OFDM symbols in an OFDM frame, based on the DPSS representation principle, we have

$$\mathbf{h}_{\text{frame}}^{(l)} = \sum_{k=0}^{B-1} g_k^{(l)} \mathbf{b}_k + \mathbf{e}^{(l)}, \quad (53)$$

where $\mathbf{h}_{\text{frame}}^{(l)}$ is the channel response corresponding to the l -th path of $\mathbf{h}_{\text{frame}}$, B is the number of DPSSs, \mathbf{b}_k is the k -th DPSS, $\mathbf{e}^{(l)}$ represents the error in the channel reconstruction using DPSS. Note that $\mathbf{h}_{\text{frame}}^{(l)}$ contains the channel responses corresponding to M OFDM symbols, and among these, we only know the values at the midpoints of M_P pilot symbols, i.e., $[h_{\text{frame}}^{(l)}[p_0], h_{\text{frame}}^{(l)}[p_1], \dots, h_{\text{frame}}^{(l)}[p_{M_P-1}]]^T$. To solve for all the coefficients $g_k^{(l)}$, it is generally required that $M_P \geq B$. Without loss of generality, we assume that $M_P = B$. Then, all the coefficients $g_k^{(l)}$ can be obtained from (54), and $\mathbf{h}_{\text{frame}}^{(l)}$ can also be calculated once $g_k^{(l)}$ is obtained, through routine calculation.

$$\eta_1(\omega_q^{(0)}, \dots, \omega_q^{(L-1)}) = \left\| \frac{1}{N} \begin{bmatrix} \sum_{k=0}^{N-1} a_k^* a_k \zeta_N^{\omega_q^{(0)} k} & \sum_{k=0}^{N-1} a_k^* a_{k-1} \zeta_N^{\omega_q^{(1)} k} & \cdots & \sum_{k=0}^{N-1} a_k^* a_{k-L+1} \zeta_N^{\omega_q^{(L-1)} k} \\ \sum_{k=0}^{N-1} a_{k-1}^* a_k \zeta_N^{\omega_q^{(0)} k} & \sum_{k=0}^{N-1} a_{k-1}^* a_{k-1} \zeta_N^{\omega_q^{(1)} k} & \cdots & \sum_{k=0}^{N-1} a_{k-1}^* a_{k-L+1} \zeta_N^{\omega_q^{(L-1)} k} \\ \vdots & \vdots & & \vdots \\ \sum_{k=0}^{N-1} a_{k-L+1}^* a_k \zeta_N^{\omega_q^{(0)} k} & \sum_{k=0}^{N-1} a_{k-L+1}^* a_{k-1} \zeta_N^{\omega_q^{(1)} k} & \cdots & \sum_{k=0}^{N-1} a_{k-L+1}^* a_{k-L+1} \zeta_N^{\omega_q^{(L-1)} k} \end{bmatrix} - \text{diag}(\mathbf{\Gamma}_q) \right\|_F^2. \quad (46)$$

$$\eta_2(\omega_q^{(0)}, \dots, \omega_q^{(L-1)}) = \left\| \frac{1}{N} \begin{bmatrix} \widetilde{AF}_{\mathbf{a}}(0, \omega_q^{(0)}) & \widetilde{AF}_{\mathbf{a}}(-1, \omega_q^{(1)}) & \cdots & \widetilde{AF}_{\mathbf{a}}(1-L, \omega_q^{(L-1)}) \\ \widetilde{AF}_{\mathbf{a}}(1, \omega_q^{(0)}) & \widetilde{AF}_{\mathbf{a}}(0, \omega_q^{(1)}) & \cdots & \widetilde{AF}_{\mathbf{a}}(2-L, \omega_q^{(L-1)}) \\ \vdots & \vdots & & \vdots \\ \widetilde{AF}_{\mathbf{a}}(L-1, \omega_q^{(0)}) & \widetilde{AF}_{\mathbf{a}}(L-2, \omega_q^{(1)}) & \cdots & \widetilde{AF}_{\mathbf{a}}(0, \omega_q^{(L-1)}) \end{bmatrix} - \text{diag}(\mathbf{\Gamma}_q) \right\|_F^2. \quad (47)$$

$$\eta_3(f) = \left\| \frac{1}{N} \left(\begin{bmatrix} \widetilde{AF}_{\mathbf{a}}(0, f) & \widetilde{AF}_{\mathbf{a}}(-1, f) & \cdots & \widetilde{AF}_{\mathbf{a}}(1-L, f) \\ \widetilde{AF}_{\mathbf{a}}(1, f) & \widetilde{AF}_{\mathbf{a}}(0, f) & \cdots & \widetilde{AF}_{\mathbf{a}}(2-L, f) \\ \vdots & \vdots & & \vdots \\ \widetilde{AF}_{\mathbf{a}}(L-1, f) & \widetilde{AF}_{\mathbf{a}}(L-2, f) & \cdots & \widetilde{AF}_{\mathbf{a}}(0, f) \end{bmatrix} - \sum_{k=0}^{N-1} \zeta_N^{fn} \mathbf{I}_L \right) \right\|_F^2. \quad (50)$$

$$\begin{bmatrix} g_0^{(l)} \\ g_1^{(l)} \\ \vdots \\ g_{B-1}^{(l)} \end{bmatrix} = \begin{bmatrix} b_0[p_0] & b_0[p_1] & \cdots & b_0[p_{M_P-1}] \\ b_1[p_0] & b_1[p_1] & \cdots & b_1[p_{M_P-1}] \\ \vdots & \vdots & & \vdots \\ b_{B-1}[p_0] & b_{B-1}[p_1] & \cdots & b_{B-1}[p_{M_P-1}] \end{bmatrix}^{-1} \begin{bmatrix} h_{\text{frame}}^{(l)}[p_0] \\ h_{\text{frame}}^{(l)}[p_1] \\ \vdots \\ h_{\text{frame}}^{(l)}[p_{M_P-1}] \end{bmatrix}. \quad (54)$$